Field-emission properties of cobalt/multiwalled carbon nanotube composite films fabricated by electrodeposition

Susumu Arai*, Kazuaki Miyagawa

Department of Chemistry and Material Engineering, Faculty of Engineering,
Shinshu University, 4-17-1 Wakasato, Nagano 380-8553, Japan

* Corresponding author
Tel: +81-26-269-5413
Fax: +81-26-269-5432
E-mail address: araisun@ shinshu-u.ac.jp (S. Arai)

Abstract

Carbon nanotubes (CNT) are promising for use as field emitters. CNT field emitters in which CNTs are attached to a cathode by a metal are highly suitable structures for CNT field emitters. In this study, cobalt (Co)/CNT composite films were fabricated by composite plating for use as field emitters. Four kinds of multiwalled CNTs (MWCNTs) with different sizes were used as CNTs. The microstructures of the composite films were examined by scanning electron microscopy. The electrical conductivity and field-emission properties of the composite films were also evaluated. Co/MWCNT composite films in which MWCNTs were homogeneously distributed were fabricated using relatively large MWCNTs. In contrast, small MWCNTs formed aggregates in the film. The composite films had lower electrical conductivities than that of a pure cobalt film. Co/MWCNT composite films exhibited obvious field emission. The Co/MWCNT composite films had field-emission electric fields in the approximate range of 1.5–2 V μm^{-1}.

Keywords: carbon nanotube; cobalt; composite; electrodeposition; field emission

1. Introduction

Carbon nanotubes (CNTs) are promising field-emission electron sources since they have high aspect ratios, very small radii of curvature, high chemical inertness, and high electrical conductivities [1, 2]. Field emitters using CNTs have been fabricated by various methods. Direct growth [3–5] permits good control of the alignment, density, diameter, and length of CNTs, but offers limited scalability in terms of substrate size and growth temperature. Screen printing [6–10] has good scalability, but outgassing from the organic vehicle in the paste degrades the CNTs. Spray deposition [11] has good scalability, but yields poor adhesion. Thus, all three methods have drawbacks for practical applications.

Recently, the field-emission properties of metal/CNT composite films fabricated by chemical displacement plating [12] and electroless composite plating [13] have been reported. We have been investigating metal/CNT composite plating. We have previously reported patterned Cu/multiwalled CNT (MWCNT) composite field emitters fabricated by electrodeposition [14] and the effects of varying the plating bath composition on the field-emission properties of Cu/MWCNT composite plating films [15]. This metal/CNT composite field emitter is expected to have several advantages. First, the CNTs are attached by a metal matrix, resulting in good adhesion. Second, it does not contain any organic substances so there will be no degradation of the CNTs. Moreover,

electroplating is inexpensive and has good scalability. However, in previous studies, we used copper as the matrix metal, which has a relatively low melting point (1096°C) for a metal. Metals with higher melting points are desirable for metal/CNT composite emitters to improve the thermal stability of the emitter during field emission. Cobalt has a relatively high melting point of 1495°C, which is 400°C higher than that of copper. Consequently, cobalt is promising as a matrix metal for metal/CNT composite field emitters.

In this study, Co/CNT composite films were fabricated and their field-emission properties were investigated.

2. Experimental

2.1. Chemicals

Four commercially available MWCNTs with different diameters were used in the present study. They are VGCF and VGCF-S (Showa Denko Co. Ltd.; diameter: 100–150 and 80 nm, respectively), MWNT-7 (Mitsui & Co., Ltd.; diameter: 60 nm), and IljinCNT (Iljin Co.; diameter: 15–20 nm). All the MWCNTs were approximately

10–15 μm long. Special grade $CoSO_4 \cdot 7H_2O$, NaCl, NaOH, and H_3BO_3 (Wako Pure Chemical Industries, Ltd.) and first grade polyacrylic acid (PA5000: Wako Pure Chemical Industries, Ltd.; mean molecular weight: 5000) were used in this study. Pure water from an electrodialysis water purifier (RFP343RA, Advantec MFS, Inc.) was used in all the experiments.

2.2. Fabrication of Co/MWCNT composite films

A solution of 1.78 M $CoSO_4 \cdot 7H_2O$ + 0.26 M NaCl + 0.57 M H_3BO_3 [16] was used as the base plating bath. The MWCNTs were hydrophobic and hence did not uniformly disperse in the base plating bath. A homogeneous dispersion of the MWCNTs was achieved by adding PA5000 to the base plating bath and stirring. The composite plating baths used had compositions of 1.78 M $CoSO_4 \cdot 7H_2O$ + 0.26 M NaCl + 0.57 M H_3BO_3 + 2.0×10^{-5} M PA5000 + x g dm^{-3} MWCNTs, where x = 1.5, 0.8, 0.55, and 0.15 for VGCF, VGCF-S, MWNT-7, and IljinCNT, respectively. Electrodeposition was performed at 50°C with agitation by bubbling air under the galvanostatic condition of 2.5 A dm^{-2}. A commercially available electrolytic cell (Model I, Yamamoto-Ms Co., Ltd.) with internal dimensions of $65 \times 65 \times 95$ mm^3 was employed for

electrodeposition. The volume of the plating bath was 300 cm^3. A pure copper plate (JIS C1201P) with an exposed surface area of 10 cm^2 (3 × 3.33 cm) was used as the cathode, while a pure cobalt plate (A-53-M1-P08-19, Yamamoto-Ms Co., Ltd.) was used as the anode.

2.3. CNT contents of Co/MWCNT composite films

The MWCNT contents of the composite films were directly determined by weighing. In the weight measurements, large amounts (over 2 g) of Co/MWCNT composite films were electrodeposited on stainless-steel substrates. After electrodeposition, the composite films were exfoliated from the stainless-steel substrates. The cobalt matrix of the composite films was dissolved in nitric acid. The MWCNTs in the nitric acid solution were filtered, dried, and weighed. The MWCNT content was calculated both as mass% and as the MWCNT number density (the number of MWCNTs per 1 g of the composite film). To calculate the MWCNT number density, the nanostructures of the MWCNTs were analyzed by scanning transmission electron microscopy (STEM; HD-2300A, Hitachi). Fig. 1 shows STEM images of the four MWCNTs used. Each MWCNT has a hollow core that is 3–6 nm in diameter. In general, MWCNTs have

cylindrical external as well as internal appearances. Consequently, each single MWCNT volume was calculated using

$$\frac{\pi}{4}\left({D_{outer}}^2 - {D_{inner}}^2\right) \times l \quad (1)$$

where π is the circular constant, D_{outer} is the outer diameter, D_{inner} is the inner diameter, and l is the length of the MWCNTs. The mass of each single MWCNT was calculated from the density of graphite (2.26 g cm^{-3}) and the number of MWCNTs per 1 g of the composite film was then calculated using the MWCNT mass% values for the composite films.

2.4. Microstructures of Co/MWCNT composite films

The surface and cross-sectional morphologies of the composite films were examined by field-emission scanning electron microscopy (JSM-7000F, JEOL Ltd.) using an acceleration voltage of 5 kV. A specially designed sample preparation system (cross-section polisher, SM-09010 JEOL Ltd.) was used to prepare cross-sectional samples for observations.

2.5. Electrical conductivities of Co/MWCNT composite films

For electrical conductivity measurements, Co/MWCNT composite films were electrodeposited on stainless-steel substrates. After electrodeposition, the composite films were exfoliated from the stainless-steel substrate and used as measurement samples. The electrical resistivities of the composite films were measured by the four-terminal method using a four-point probe system.

2.6. Field-emission properties of Co/MWCNT composite films

The field-emission properties of the composite films were measured using a diode-type field-emission measurement system (CN-EMS30, Ulvac Inc.). The base pressure of the field-emission chamber was about 10^{-5} Pa. The composite film cathodes had dimensions of 3 cm × 3.3 cm. A cylindrical stainless-steel electrode with a surface area of 0.785 cm^2 was used as the anode. There was a 1 mm gap between the anode and the composite film surface. The emission current density was calculated by dividing the measured emission current by the anode surface area (0.785 cm^2).

3. Results and discussion

3.1. Surface and cross-sectional morphologies of Co/MWCNT composite films

Fig. 2 shows SEM images of the surfaces of the electrodeposited Co/MWCNT composite films. It shows that MWCNTs are homogeneously distributed in the Co/VGCF (Fig. 2a), Co/VGCF-S (Fig. 2b), and Co/MWNT-7 (Fig. 2c) composite films. Therefore, MWCNTs should be homogeneously dispersed in the plating baths used to prepare these films without forming aggregates. In contrast, MWCNTs aggregated in the Co/IljinCNT composite film (Fig. 2d). IljinCNTs are the smallest of the four MWCNTs used in this study. Consequently, the cohesive force between individual CNTs will be strong. Since the IljinCNTs were not sufficiently well dispersed in the plating bath, they formed aggregates in the composite film. However, aggregates of IljinCNTs were homogeneously distributed in the composite film. In previous studies of Cu/MWCNT [17] and Ni/MWCNT [18] composite plating, we found that metal particles are readily electrodeposited on the edges or defect sites of the MWCNT walls during composite plating due to the high electrical conductivity of the MWCNTs along

their axis. However, cobalt particles were not observed on every MWCNT in the present study. This morphology is desirable for field emission because MWCNTs have very small radii of curvature. Fig. 3 shows cross-sectional SEM images of the composite films. The dark regions are cross sections of MWCNTs. MWCNTs are observed in the cobalt matrix of all the composite films, which indicates that all four MWCNTs were incorporated in the composite films. In other words, MWCNTs are strongly attached to the cobalt metal. Furthermore, the composite films are thought to have compact structures since the films do not contain any gaps or voids. MWCNTs are individually distributed in the case of Co/VGCF, Co/VGCF-S, and Co/MWCNT-7 composite films (Figs. 3a–3c), whereas MWCNT aggregates are observed in the Co/IljinCNT composite film (Fig. 3d). These results indicate that the cross sections have the same microstructures as the surfaces.

3.2. MWCNT contents of composite films

Table 1 lists the MWCNT contents of the composite films. The content is indicated both in terms of mass% and the MWCNT number density. The MWCNT content of the Co/VGCF composite film of 0.51 mass% is three to four times higher than those of the

other three composite films, which have similar MWCNT contents (0.13–0.17 mass%). The MWCNT number density for the Co/IljinCNT composite film (2.0×10^{11}) is over 10 times larger than those of the other three composite films, which have similar values as each other ($1.0–1.7 \times 10^{10}$). The number of MWCNTs at the surfaces of the composite films is expected to affect the field-emission properties of the films. In this study, the number of MWCNTs at the surfaces of the composite films was not directly evaluated. However, since the MWCNTs are homogeneously distributed across the composite films (while IljinCNTs form aggregates, these aggregates are homogeneously distributed), as shown in Figs. 2 and 3, the MWCNT number density should reflect the number of MWCNTs at (on) the surfaces of the composite films.

3.3. Electrical resistivities of Co/MWCNT composite films

Table 2 lists the electrical resistivities of the four films. The field-emission properties, especially the field-emission electric field (the turn-on electric field), improve with decreasing electrical resistivity (increasing electrical conductivity) of the composite films. The pure cobalt film electrodeposited from the above-described base plating bath had an electrical resistivity of 8.5 μΩ cm. The Co/MWCNT composite films had higher

electrical resistivities than the pure cobalt film. The electrical resistivity of an individual MWCNT has not been accurately determined. If all the MWCNTs have the same resistivity as graphite of about 100 μΩ cm, it will be over 10 times higher than that of pure cobalt film. Furthermore, the PA5000 dispersant may be incorporated as an impurity in the composite films during electrodeposition. This may contribute to the Co/MWCNT composite films having higher resistivities than the pure cobalt film. However, since the composite films do not have very high resistivities, the field-emission properties are not expected to be greatly affected by the resistivity of the composite films.

3.4. Field-emission properties of Co/MWCNT composite films

Fig. 4 shows the field-emission properties of the four films. No emission current was detected from the pure cobalt film. In contrast, apparent emission currents were measured for all the Co/MWCNT composite films. Therefore, the MWCNTs in the composite films are thought to act as electron emitters. The field-emission current density J can generally be expressed as a function of the external electric field E by the Fowler–Nordheim equation [19, 20]:

$$J = \frac{e^3 E^2}{8\pi h \phi t^2(y)} \exp\left[\frac{-8\pi(2m)^{1/2}\phi^{3/2}}{3heE} v(y)\right] \quad (2)$$

where e is the elementary charge, h is Planck's constant, f is the work function of the sample, m is the electron mass, and $t(y)$ and $v(y)$ are the Nordheim elliptic functions. Transforming Eq. 2, we obtain

$$\ln\left(\frac{I}{V^2}\right) = -\frac{b}{V} + \ln a \quad (3)$$

where I is the emission current, V is the voltage, and a and b are constants. Therefore, if the experimentally measured electron emission current (I) against the applied voltage (V) in Fowler–Nordheim coordinates (i.e., $\ln(I/V^2)$ vs. $1/V$) is linear with a negative slope, the measured emission current of the sample will be the field-emission current. Fig. 5 shows the corresponding Fowler–Nordheim plots. Since these plots are almost linear, the measured currents are considered to be field-emission currents. In other words, the Co/MWCNT composite films are field emitters. In this study, the turn-on electric field is defined as the electric field corresponding to an emission current density of 10 nA cm^{-2}. The turn-on electric field is considered to be affected by the radius of

curvature of the MWCNTs (i.e., the MWCNT diameter). From Fig. 4, the turn-on electric fields of Co/VGCF, Co/VGCF-S, Co/MWNT-7, and Co/IljinCNT composite films are 1.9, 1.8, 1.6, and 1.6 V μm^{-1}, respectively. Thus, the turn-on electric fields of the composite films tend to decrease with decreasing MWCNT diameter. Since the IljinCNTs have the smallest diameter, the Co/IljinCNT composite film is expected to exhibit a lower turn-on electric field than the Co/MWNT-7 composite film. As shown in Fig. 2d, the IljinCNTs exist as aggregates in the composite film. Some IljinCNTs may form bundles. Therefore, the actual radius of curvature of the IljinCNTs may be larger than that of individual MWCNTs, which would cause the turn-on electric field to be higher than expected. As for the current density, a composite film containing a larger number of MWCNTs is expected to exhibit a higher current density. Fig. 4 shows that the Co/MWNT-7 and Co/IljinCNT composite films have the highest and lowest current densities, respectively. As shown in Table 1, the Co/IljinCNT composite film has the largest number of MWCNTs in the composite film so that it is expected to exhibit the highest current density. However, as mentioned above, the IljinCNTs form aggregates; this may reduce the number of MWCNTs available for field emission and thereby reduce the current density. On the other hand, Co/MWNT-7 composite film has the second largest number of MWCNTs (Table 1) and the MWCNTs are homogeneously

distributed in the composite film. Consequently, the Co/MWNT-7 composite film showed the highest current density among the Co/MWCNT composite films.

4. Conclusions

Co/MWCNT composite films were fabricated by electrodeposition using four kinds of MWCNTs that have different diameters. The Co/MWCNT composite films showed apparent field emission with relatively low field-emission electric fields in the range 1.5–2.0 V μm^{-1}. Co/MWCNT composite films, which have a high melting point matrix, are expected to be useful as thermally stable field emitters for field-emission devices such as field-emission displays.

References

[1] A.G. Rinzler, J.H. Hafner, P. Nikolaev, L. Lou, S.G. Kim, D. Tomanek, P. Nordlander, D.T. Colbert, R.E. Smally, Science 269 (1995) 1550–1553.

[2] W.A. de Heer, A. Chatelain, D. Ugarte, Science 270 (1995) 1179–1180.

[3] J.I. Sohn, S. Lee, Appl. Phys. Lett. 78 (2001) 901–903.

[4] Y. Huh, J.Y. Lee, C.J. Lee, Thin Solid Film 475 (2005) 267–270.

[5] M.P. Siegal, P.A. Miller, P.P. Provencio, D.R. Tallant, Diamond Relat. Mater. 16 (2007) 1793–1798.

[6] W.B. Choi, D.S. Chung, J.H. Kang, H.Y. Kim, Y.W. Jin, I.T. Han, Y.H. Lee, J.E. Jung, N.S. Lee, G.S. Park, J.M. Kim, Appl. Phys. Lett. 75 (1999) 3129–3131.

[7] W.J. Zhao, A. Sawada, M. Takai, Jpn. J. Appl. Phys. 41 (2002) 4314–4316.

[8] J. Li, W. Lei, X. Zhang, X. Zhou, Q. Wang, Y. Zhang, B. Wang, Appl. Surf. Sci. 220 (2003) 96–104.

[9] H.J Lee, Y.D. Lee, S.I. Moon, W.S. Cho, Y.H. Lee, J.K. Kim, S.W. Hwang, B.K. Ju, Carbon 44 (2006) 2625–2630.

[10] C.W. Cheng, C.M. Chen, T.C. Lee, Appl. Surf. Sci. 255 (2009) 5770–5774.

[11] Y.D. Lee, K.S. Lee, Y.H. Lee, B.K. Ju, Appl. Surf. Sci. 254 (2007) 513–516.

[12] Y.C. Fan, Y.M. Liu, Y.C. Chen, Y. Sung, M.D. Ger, Appl. Surf. Sci. 255 (2009) 7753–7758.

[13] B.R. Huang, T.C. Lin, Y.K. Yang, S.D. Tzeng, Diamond Relat. Mater. 19 (2010) 158–161.

[14] S. Arai, T. Saito, M. Endo, Electrochem. Solid-State Lett. 11 (2008) D72–D74.

[15] S. Arai, T. Saito, M. Endo, J. Electrochem. Soc. 157 (2010) D127–D134.

[16] E.C. Kedward, C.A. Addison, A.A.B. Tennett, Trans. Inst. Metal Finishing 54 (1976) 8–10.

[17] S. Arai, M. Endo, Electrochem. Commun. 5 (2003) 797–799.

[18] S. Arai, M. Endo, N. Kaneko, Carbon 42 (2004) 641–644.

[19] R.H. Fowler, D.L. Nordheim, Roy. Soc. Proc. A173 (1928).

[20] D. Temple, Mater. Sci. Eng. R 24 (1999) 185–239.

Figure captions

Fig. 1 STEM images of various MWCNTs: (a) VGCF, (b) VGCF-S, (c) MWNT-7, and (d) IljinCNT.

Fig. 2 Surface SEM images of electrodeposited Co/MWCNT composite films: (a) Co/VGCF, (b) Co/VGCF-S, (c) Co/MWNT-7, and (d) Co/IljinCNT composite films.

Fig. 3 Cross-sectional SEM images of electrodeposited Co/MWCNT composite films: (a) Co/VGCF, (b) Co/VGCF-S, (c) Co/MWNT-7, and (d) Co/IljinCNT composite films.

Fig. 4 Field-emission properties of ○ pure cobalt film and of □ Co/VGCF, △ Co/VGCF-S, ◎ Co/MWNT-7, and ◇ Co/IljinCNT composite films.

Fig. 5 Fowler–Nordheim plots of ○ pure cobalt film and of □ Co/VGCF, △ Co/VGCF-S, ◎ Co/MWNT-7, and ◇ Co/IljinCNT composite films.

Table captions

Table 1 MWCNT contents of Co/MWCNT composite films.

Table 2 Electrical resistivities of various films.

Figure(1)

Click here to download Figure(s): Figure1.pptx

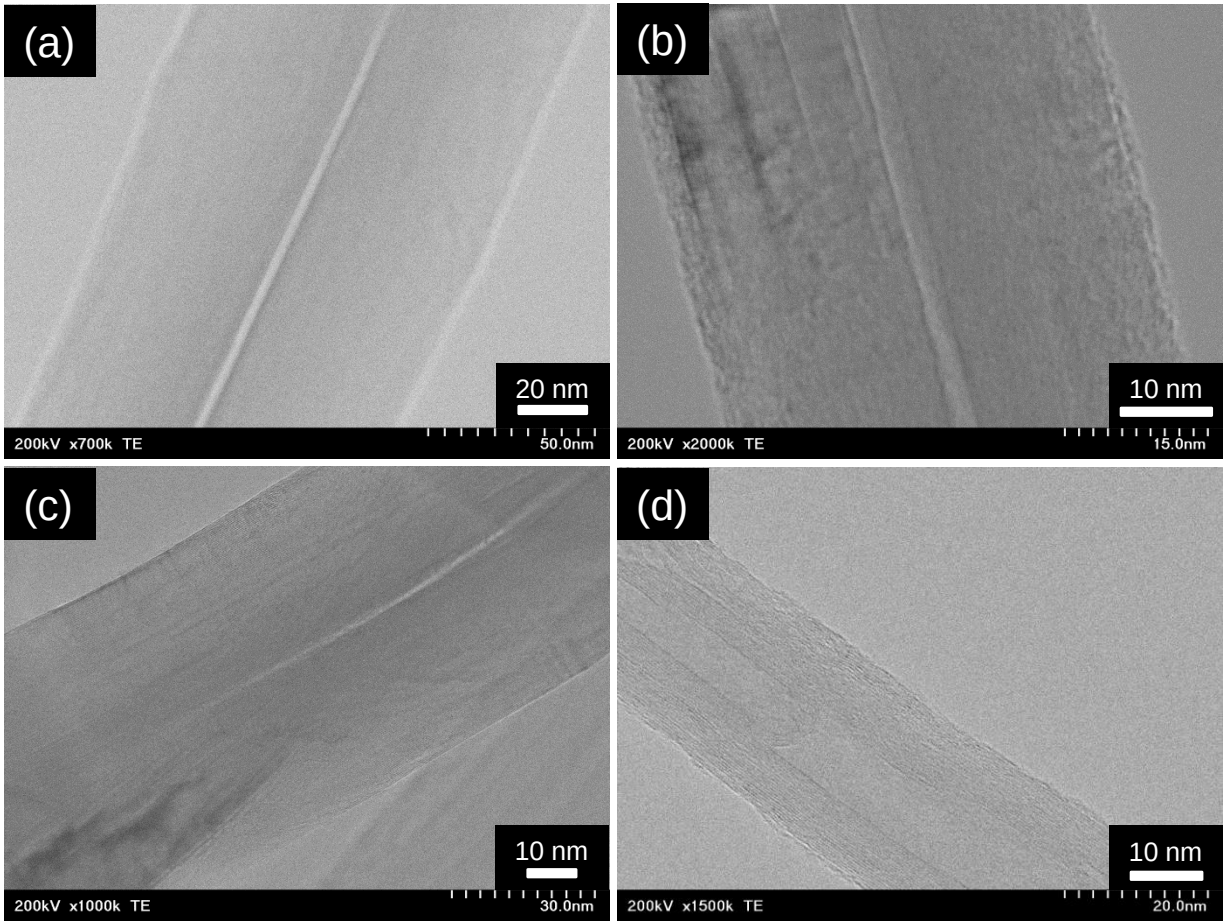

Fig.1

Figure(2)

Click here to download Figure(s): Figure2.pptx

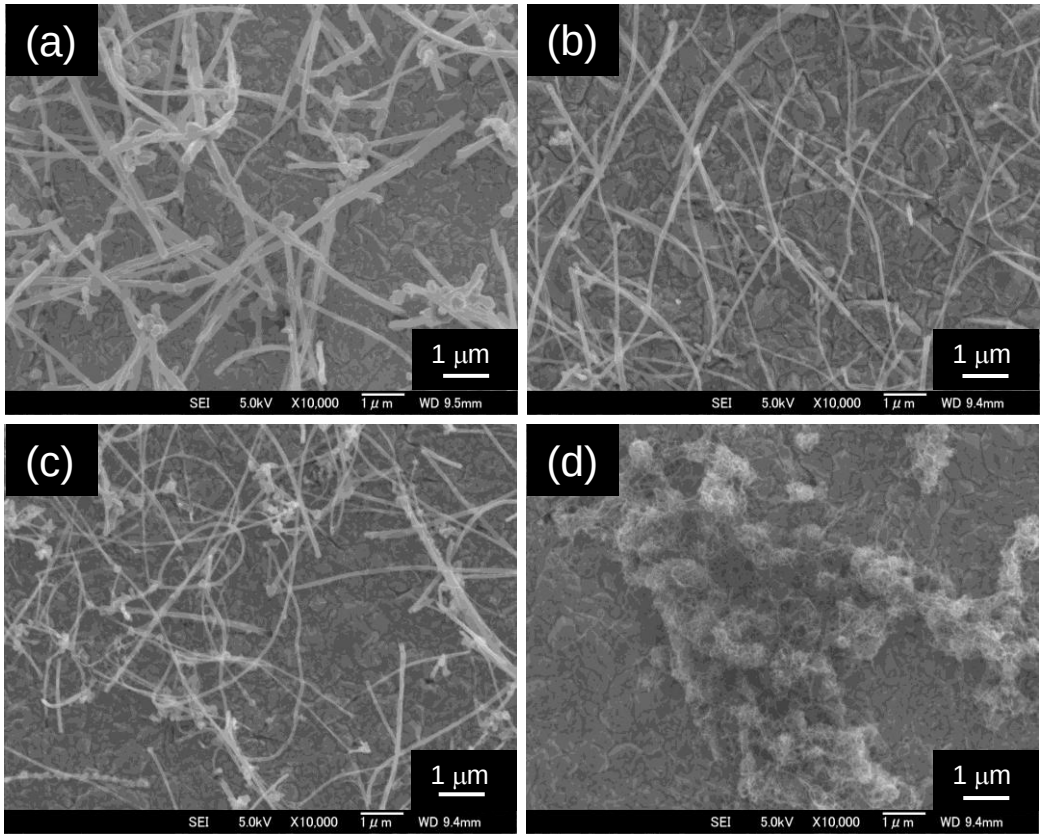

Fig.2

Figure(3)
Click here to download Figure(s): Figure3.pptx

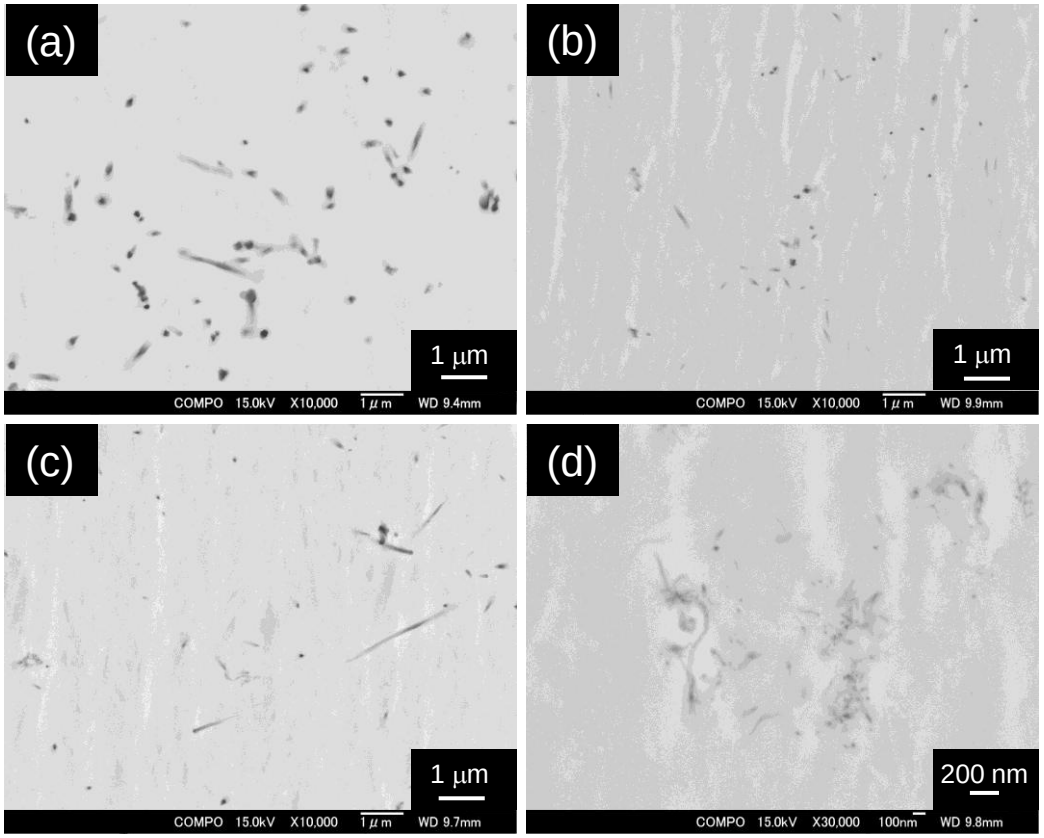

Fig.3

Figure(4)

Click here to download Figure(s): Figure4.pptx

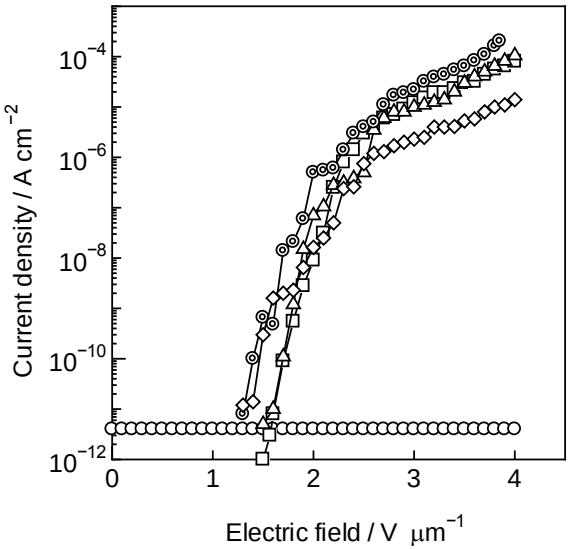

Fig.4

Figure(5)

Click here to download Figure(s): Figure5.pptx

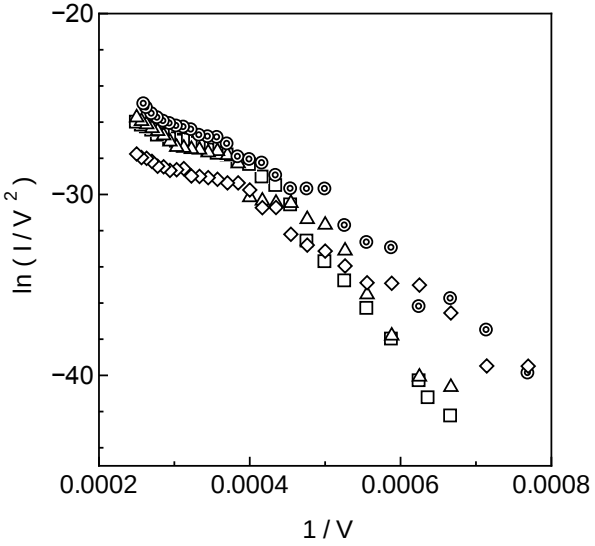

Fig.5

Table(1)

Table 1

Co/MWCNT composite film	Mass%	MWCNT number density (MWCNT number / g)
Co/VGCF composite film	0.51	1.2×10^{10}
Co/VGCF-S composite film	0.17	1.0×10^{10}
Co/MWNT-7 composite film	0.15	1.7×10^{10}
Co/IljinCNT composite film	0.13	2.0×10^{11}

Table(2)

Table 2

Co/MWCNT composite film	Electrical resistivity (μΩ cm)
Cobalt film	8.5
Co/VGCF composite film	13.1
Co/VGCF-S composite film	15.2
Co/MWNT-7 composite film	14.9
Co/IljinCNT composite film	16.2